ERT AND GPR WATERBORNE SURVEYS ON A HIGH-ELEVATION ALPINE POND (NW ITALY)

L. Sambuelli[1], C. Comina[2], C. Colombero[1], V.J. Rumbos Ruedas[1], C. De Regibus[1], N. Colombo[3], M. Freppaz[3]

[1] DIATI, Politecnico di Torino, Italy
[2] DST, Università di Torino, Italy
[3] DISAFA, Università di Torino, Italy

Introduction. High-elevation lakes are a common feature of mountain environments and play an important role in the hydrological and chemical dynamics of mountain watersheds (e.g., Catalan *et al*., 2006; Salerno *et al*., 2014). These lakes are also recognised as key reference freshwater sites for global scale processes, due to the lack of direct human influence and because their physical, chemical, and biological properties respond rapidly to climate changes (e.g., Carpenter *et al*., 2007; Lami *et al*., 2010). Usually, water bodies located in high mountain environments are characterised by small dimensions, and can be defined as ponds (Hamerlík *et al*., 2014). Their relatively low water volumes and high surface area to depth ratios make these features more fragile (Buraschi *et al*., 2005). Moreover, high-elevation lakes and ponds are often located in basins characterised by the permafrost presence; the degradation of permafrost has been reported to deeply impact the surface water quality (Colombo *et al*., 2018a). Thus, high-elevation ponds should be considered as key "field" laboratories for the study of climate change impacts on aquatic ecosystems. In this context, waterborne geophysical methods can map hydrogeological information, correlating geophysical parameters to hydrological and geological properties (Colombero *et al*., 2014; Colombo *et al*., 2018b), and deriving fundamental information for further investigations such as hydrochemical analyses (Colombo *et al*., 2018c).

In this work, we present the results of waterborne ground penetrating radar (GPR) and electrical resistivity tomography (ERT) on the Bowditch Pond, a high-elevation pond located in NW Italian Alps.

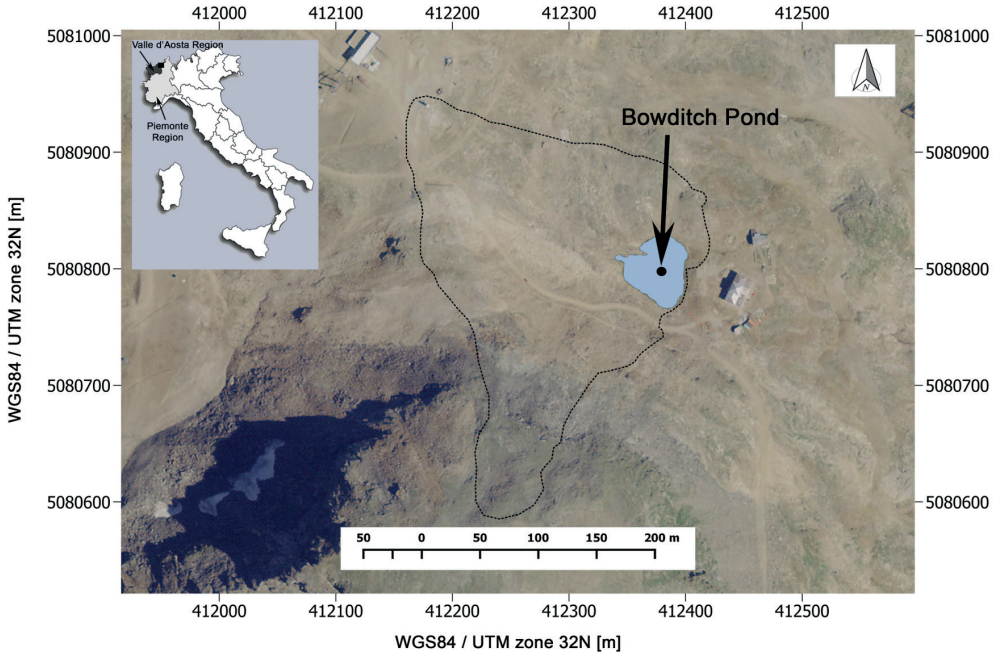

Fig. 1 - Location of the study area in Italy and overview of the investigated pond basin (Digital orthoimage year 2006, source: Ministero dell'Ambiente e della Tutela del Territorio e del Mare - Geoportale Nazionale, http://www.pcn.minambiente.it/GN). The black dashed line indicates the basin border.

Study area. The Bowditch Pond (elevation: 2901 m a.s.l., area: 2405 m^2) is located in a small valley depression in the uppermost area of the Cimalegna glacial plateau, in the Piemonte Region, close to the border with the Valle d'Aosta Region (Fig. 1). The pond has no persistent surface inflows while a surface outflow is present, although it usually disappears during the ice-free season (August). Permafrost is likely to exist in the basin (Boeckli *et al*., 2012). The water basin is mainly surrounded by coarse debris deposits of various rock types outcropping in the surroundings, belonging to different overlapping tectono-metamorphic units, and varying from micaschists and gneisses, with acid composition and schistous and massive structure, to eclogites, amphibolites, and other rock types with basic composition. In particular, the northern shore of the pond is characterized by garnet-bearing micaschists with embedded eclogitic lenses and a big quartz vein. To the NW of the pond, an elongated ridge of compact rock is present. The latter is composed of garnet-bearing micaschists. Eclogites are outcropping to the East and micaschists with no evident garnet content are present along the south-western shore. The complex geo-structural background of the pond surroundings is complicated and partially hidden by the presence of fractured rocks and coarse debris covers.

Data acquisition. Extensive waterborne GPR profiles and ERT lines were acquired on the Bowditch Pond. An IDS 200-MHz bistatic antenna placed at the bottom of a plastic inflatable boat and controlled by an IDS K2 digital acquisition unit was used for waterborne GPR profiling. The boat was driven by an electric engine to maintain a constant speed and an Ublox EVK-5T GPS was used to track the survey position. GPR profiles were densely acquired following different directions in order to sufficiently cover the pond area in two subsequent campaigns. In the first survey, 19 profiles were acquired with a time increment of 0.48 ns and 1024 samples per trace, for a total time of 500 ns; in the second one, 17 profiles were recorded with the same time increment, 2048 sample per trace and a trace duration of 1000 ns. On the whole, we acquired 1331.2 m of GPR profiles (Fig. 2). By contrast, waterborne electrical profiling with towed floating cables was not possible due to the small area of the pond. As a consequence,

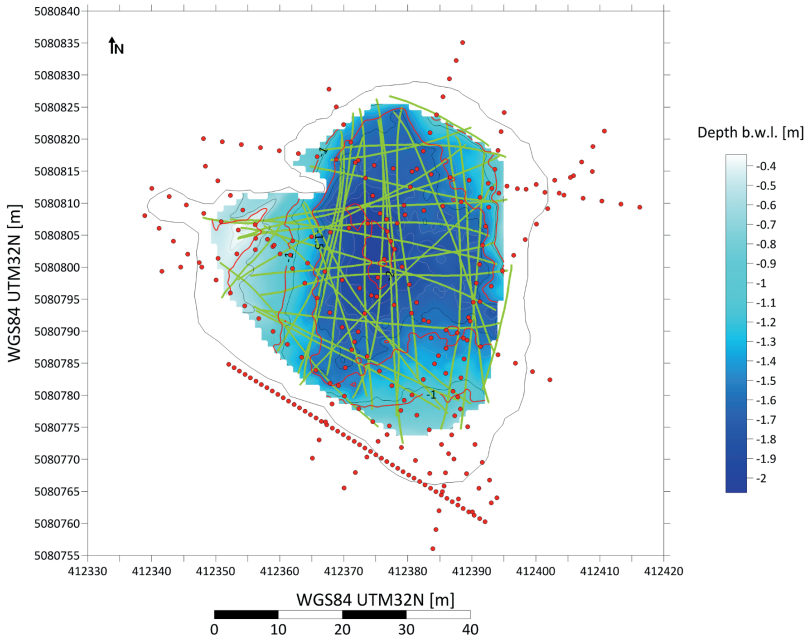

Fig. 2 - Location of the geophysical survey and bathymetry contour map of the pond reconstructed from GPR data. The pond perimeter is marked with a black line. Green lines trace the waterborne GPR profiles. Yellow dots refer to the electrode locations of the 10 ERT lines (9 lines with 24 electrodes at 3-m spacing + 1 line with 48 electrodes at 1-m spacing).

ERT lines with floating cables, having equi-spaced electrode locations, were stretched across the pond. Polyethylene foam floaters were used to maintain the cable at the water surface, but ensuring the cable takeout (directly used as electrodes) to be submerged. At the ERT line edges, the cable takeouts were connected to stainless steel electrodes fixed in the ground of the pond shore. A total of 9 ERT profiles were acquired on the pond, with 24 electrodes at 3-m spacing. An additional line, with 48 electrodes at 1-m spacing, was additionally acquired close to the southern shore of the pond (Fig. 2). The first and last electrodes of each line were geo-referenced using a Garmin GPS 60 to retrieve the position of each survey line. A Wenner-Schulumberger acquisition sequence was adopted, using a multichannel resistivity system (Syscal Pro - Iris Instruments). Before each current injection, the natural Spontaneous Potential (SP) between each current dipole was additionally recorded.

Data processing. GPR data processing consisted of i) trace regularization, on the basis of the effective profile length and number of traces; ii) time cut, to reduce the trace length after a check of the deterioration of the S/N ratio; iii) move start time, to remove the delay introduced by the system; iv) dewow, to reduce very low frequency components; v) further time cut, to equalize the sample number within the traces of the two surveys; vi) divergence compensation, to increase deep echoes strength; vii) subtracting average, to remove horizontal bands and viii) muting above the pond-bed picking. No clear velocity domains were found to migrate the many diffraction hyperbola present in the radargrams. The manual picking of the pond bottom on the radargrams was further used to reconstruct the pond bathymetry. Given the density of the GPR traces, retrieved water depths were then interpolated over the surveyed area to obtain a reference bathymetry map (Fig. 2).

Electrical profiles were processed with both 2-D and 3-D inversion procedures. Raw apparent resistivity measurements were filtered basing on their related standard deviation (each measurement is the average of 10 subsequent measures) to improve the overall data quality. Measurements with standard deviation higher than 1% were filtered out from the dataset. Two different 2-D robust inversions were performed on each ERT profile (Res2DInv, Geotomo): the first not introducing a-priori information on the water layer; the second constraining the bathymetry of the pond (from GPR data) and the water resistivity (fixed to 125 Ohm m, as obtained from independent in-situ measurements with a portable conductimeter). The 3-D inversion was carried out without a-priori constraints (ERTLab, Geostudi). The SP measurements related to the dipoles with lower spacing were also extracted and mapped over the pond. Each SP measure was plotted in the centre of the measuring dipole. Minimum distance between two current electrodes (AB) was 9 m, consequently raw SP data are approximately related to a depth of investigation of around 4.5 m (AB/2). This depth corresponds to the first 2-3 m below the pond bottom and may be diagnostic of recharge (positive SP anomaly) or seepage (negative SP anomaly) hydrodynamic processes occurring at the pond bottom.

Results and discussions. The bathymetry map obtained from GPR data processing (Fig. 2 and 3) highlighted tiny water depths over the investigated area, with a maximum of approximately 2 m in the centre of the pond. The majority of the diffraction hyperbolas observed in the radargrams were due to the widespread presence of schist slabs and decimetric blocks laying on the pond bottom. These hyperbolas showed asymptote slopes tending to 0.03 m/ns, i.e. the radar propagation velocity in water. Nevertheless, other diffraction hyperbolas showing higher velocities (around 0.05 m/s) were also noticed and not so clearly interpretable. Only in restricted parts of the pond bottom, thin decimetric layers of lacustrine sediments were found. As a consequence, it is unlikely that the aforementioned anomalous diffractions were due to blocks or slabs within the sediments. Apart from the blocks sliding within the pond from the lateral debris covers, the sedimentation of finer materials within the basin is almost negligible and the pond seems to directly lie on a rocky bedrock or on very coarse debris bodies. In this respect, ERT results (Fig. 3) highlighted a submerged high-resistivity promontory, elongating from the SW to the NE of the pond. The morphology of this body is highlighted with the

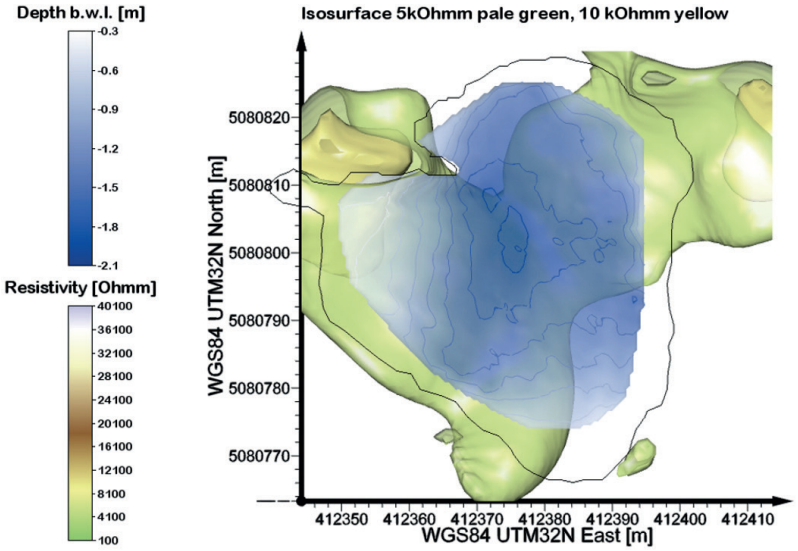

Fig. 3 - Results of the 3D inversion of the 10 ERT profiles: isosurface at 5 kOhm m (in green) and 10 kOhm m (in yellow). The pond bathymetry obtained from GPR is overlapped with the white-blue color scale. The pond perimeter is highlighted with the black line.

isosurface of electrical resistivity values higher than 5 kOhm m (Fig. 3, in green). Given the resistivity values, this promontory can be likely interpreted as the submerged and buried prosecution of the compact rocky edge outcropping on the western shore of the pond. The areas of the pond bottom outside this isosurface (N and S edges of the pond) can be likely composed of more fractured bedrock or coarse debris bodies. Within the promontory, some areas with even higher resistivity values (>10 kOhm m, Fig. 3, in yellow) were found to the NE and NW of the pond perimeter. These extremely high resistivity values have been attributed in literature to the presence of permafrost or ice bodies (e.g. Schrott and Sass, 2008). These high-resistivity regions correspond to negative SP anomalies (-10 mV to -25 mV), while a global positive SP distribution is found in the central part of the pond (0 mV to 25 mV). The interpretation of the overall electrical parameter distribution, as well as the acquired radargrams, is still debated and under investigation.

Acknowledgements. We would like to thank Consorzio di Miglioramento Fondiario di Gressoney (Aosta) and MonteRosa-ski. This research has been partially developed in the European Regional Development Fund in Interreg Alpine Space project Links4Soils (ASP399): Caring for Soil-Where Our Roots Grow (http://www.alpine-space.eu/projects/links4soils). The Authors would like to thank the management of the "Rifugio Gabiet" for their warm attitude with the field crew.

References

Boeckli, L., Brenning, A., Gruber, S., Noetzli, J.; 2012: Permafrost distribution in the European Alps: calculation and evaluation of an index map and summary statistics, The Cryosphere, 6, 807-820.

Buraschi, E., Salerno, F., Monguzzi, C., Barbiero, G., Tartari, G.; 2005: Characterization of the Italian lake-types and identification of their reference sites using anthropogenic pressure factors, Journal of Limnology, 64(1), pp. 75-84.

Catalan, J., Camarero, L., Felip, M., Pla, S., Ventura, M., Buchaca, T., Bartumeus, F., de Mendoza, G., Miró, A., Casamayor, E.O., Medina-Sánchez, J.M., Bacardit, M., Altuna, M., Bartrons, M., De Quijano, D.D.; 2006: High mountain lakes: Extreme habitats and witnesses of environmental changes, Limnetica, 25(1-2), pp 551-584.

Carpenter, S.R., Benson, B.J., Biggs, R., Chipman, J.W., Foley., J.A., Golding, S.A., Hammer, R.B., Hanson, P.C., Johnson, P.T.J., Kamarainen, A.M., Kratz, TK., Lathrop, R.G., McMahon, K.D., Provencher, B., Rusak, J.A., Solomon, C.T., Stanley, E.H., Turner, M.G., Vander Zanden, J.M., Wu, C-H., Yuan, H.; 2007: Understanding regional change: A comparison of two lake districts, Bioscience, 57, pp. 323-335.

Carrivick J. L. and Tweed F. S.; 2013: Proglacial lakes: character, behavior and geological importance, Quaternary Science Review, 78, pp. 34-52.

Colombero, C., Comina, C., Gianotti, F. and Sambuelli L.; 2014: Waterborne and on-land electrical surveys to suggest the geological evolution of a glacial lake in NW Italy, Journal of Applied Geophysics, 105, pp. 191-202.

Colombo, N., Salerno, F., Gruber, S., Freppaz, M., Williams, M., Fratianni, S., Giardino, M.; 2018a: Review: impacts of permafrost degradation on inorganic chemistry of surface fresh water, Global and Planetary Change, 162, pp. 69-83.

Colombo, N., Sambuelli, L., Comina, C., Colombero, C., Giardino, M., Gruber, S., Viviano, G., Vittori Antisari, L., Salerno, F.; 2018b: Mechanisms linking active rock glaciers and impounded surface water formation in high-mountain areas. Earth Surface Processes and Landforms, 43(2), pp. 417-431.

Colombo, N., Gruber, S., Martin, M., Malandrino, M., Magnani, A., Godone, D., Freppaz, M., Fratianni, S., Salerno, F.; 2018c: Rainfall as primary driver of discharge and solute export from rock glaciers: The Col d'Olen Rock Glacier in the NW Italian Alps, Science of the Total Environment, 639, pp. 316-330.

Hamerlík, L., Svitok, M., Novikmec, M., Očadlík, M., Bitušík, P.; 2014: Local, among-site, and regional diversity patterns of benthic macroinvertebrates in high altitude waterbodies: Do ponds differ from lakes? Hydrobiologia, 723(1), pp. 41-52.

Lami, A., Marchetto, A., Musazzi, S., Salerno, F., Tartari, G., Guilizzoni, P., Rogora, M., Tartari, G.A; 2010: Chemical and biological response of two small lakes in the Khumbu Valley, Himalayas (Nepal) to short-term variability and climatic change as detected by long-term monitoring and paleolimnological methods, Hydrobiologia, 648, pp. 189-205.

Salerno, F., Gambelli, S., Viviano, G., Thakuri, S., Guyennon, N., D'Agata, C., Diolaiuti, G., Smiraglia, C., Stefani, F., Bocchiola, D., Tartari, G.; 2014: High alpine ponds shift upwards as average temperatures increase: A case study of the Ortles-Cevedale mountain group (Southern Alps, Italy) over the last 50 years, Global and Planetary Change, 120, pp. 81-91.

Schrott, L., Sass, O.; 2008: Application of field geophysics in geomorphology: Advances and limitations exemplified by case studies, Geomorphology, 93, pp. 55-73